processes

MDPI

Article

Assessment of Organic and Inorganic Waste Suitability for Functionalization with Aminosilanes: A Comparative Study of APTMS and PEI

Mariana G. Peña-Juarez [1], Angelica M. Bello [2,*], Albino Martinez-Sibaja [2,*], Rubén Posada-Gómez [1], José P. Rodríguez-Jarquin [2] and Alejandro Alvarado-Lassman [2]

[1] SECIHT/Tecnológico Nacional de México, CRODE de Orizaba, Orizaba 94300, Veracruz, Mexico; mariana.pj@orizaba.tecnm.mx (M.G.P.-J.); ruben.pg@orizaba.tecnm.mx (R.P.-G.)
[2] Tecnológico Nacional de México, Instituto Tecnológico de Orizaba, Orizaba 94300, Veracruz, Mexico; jose.rj@orizaba.tecnm.mx (J.P.R.-J.); alejandro.al@orizaba.tecnm.mx (A.A.-L.)
* Correspondence: mara.br@orizaba.tecnm.mx (A.M.B.); albino.ms@orizaba.tecnm.mx (A.M.-S.)

Abstract

Waste materials have emerged as attractive low-cost feedstocks for adsorbent development in environmental remediation and materials engineering. Organic wastes are particularly rich in cellulose, hemicellulose, lignin, and pectin, which provide reactive oxygenated groups such as hydroxyls and carboxyls. While inorganic wastes offer stability, lower water retention makes them promising candidates. This study explores the functionalization of waste-derived organic and inorganic matrices using two amine-based agents: 3-aminopropyltrimethoxysilane (APTMS) and polyethylenimine (PEI). The materials were categorized as organic (orange peel, corn cob) or inorganic (silica gel, eggshell) and subjected to a pretreatment process involving drying, grinding, and sieving; inorganic substrates additionally underwent acid activation with citric acid. Surface modification was carried out in ethanolic (APTMS) or aqueous (PEI) media. To assess their suitability and processability as particulate sorbents, drying kinetics, physicochemical properties (FTIR, ζ-potential, pH, conductivity, Boehm titration), and flow characteristics (Carr and Hausner indices) were evaluated. The findings enable a comparative analysis of the functionalization efficiency and elucidate the relationship between substrate type (organic vs. inorganic) and its performance as a modified adsorbent. This approach advances the development of novel sorbent matrices for greenhouse gas mitigation while reinforcing circular economy principles through the valorization of low-cost, readily available waste materials.

Keywords: CO_2 capture; waste valorization; amine functionalization; organic and inorganic waste

check for updates

Academic Editors: Lucian-Ionel Cioca and Elena Simina Lakatos

Received: 1 September 2025
Revised: 25 September 2025
Accepted: 26 September 2025
Published: 29 September 2025

Citation: Peña-Juarez, M.G.; Bello, A.M.; Martinez-Sibaja, A.; Posada-Gómez, R.; Rodríguez-Jarquin, J.P.; Alvarado-Lassman, A. Assessment of Organic and Inorganic Waste Suitability for Functionalization with Aminosilanes: A Comparative Study of APTMS and PEI. *Processes* **2025**, *13*, 3117. https://doi.org/10.3390/pr13103117

Copyright: © 2025 by the authors. Licensee MDPI, Basel, Switzerland. This article is an open access article distributed under the terms and conditions of the Creative Commons Attribution (CC BY) license (https://creativecommons.org/licenses/by/4.0/).

1. Introduction

Adsorption processes represent a versatile and widely applied strategy in separation, purification, and environmental engineering and materials science due to their efficiency, operational simplicity, and scalability. The efficiency of adsorption depends not only on the intrinsic chemical affinity of the adsorbent but also on its physicochemical and handling properties, such as surface functional groups, moisture retention, flowability, and performance in packed-bed configurations [1,2]. Among different materials vastly used as sorbent materials, mesoporous silicas and MOFs offer high surface areas and tunable porosity, yet their synthesis typically involves solvothermal methods that are difficult to

scale sustainably [3,4]. Zeolites, known for their selectivity and structural stability, also demand extreme processing conditions, often reliant on fossil fuels. In response to these limitations, circular economy principles have inspired the repurposing of organic and inorganic waste materials as low-impact adsorbents [3]. This strategy not only diverts waste from landfills but also reduces reliance on virgin resources, aligning with Sustainable Development Goals (SDGs) 12 and 13 [5,6].

Organic wastes such as fruit peels and lignocellulosic residues possess inherent adsorptive properties due to their cellulose, hemicellulose, lignin, and pectin content [7]. These components provide oxygenated groups (hydroxyls, carboxyls) that enable chemical modification and functionalization. Inorganic wastes, including spent silica and eggshell (primarily calcium carbonate), offer greater dimensional stability, lower water retention, and surfaces dominated by carbonate or silanol groups. Both inorganic and organic waste present characteristics that make them promising candidates for direct functionalization while maintaining mechanical robustness [8].

Despite their potential, many waste-derived substrates exhibit limited initial performance due to intrinsic characteristics [9]. Organic waste, due to its hydrophilic nature, tends to have high moisture retention and slow kinetics; in contrast, inorganic waste may exhibit low surface reactivity due to the saturation/scarcity of active sites and, therefore, requires prior activation [8,10]. And both can present low selectivity or affinity to the material to absorption processes. To address this, it is necessary to find a surface activation that exposes the functional groups such as hydroxyl (–OH) and carboxyl (–COOH) groups that facilitate subsequent chemical modification [8,9]. These activated sites serve as anchors for agents that improve selectivity during the adsorption process. Another important factor is the type of waste. Since inorganic waste does no present active sites, it is necessary to utilize acid activation by using green agents such as citric acid that can expose -OH and carboxyl groups on their surface [9].

Selective amine functionalization, particularly with compounds such as 3-aminopropyltrimethoxysilane (APTMS) and polyethylenimine (PEI), has been widely adopted to increase both affinity and adsorption efficiency, especially for CO_2 greenhouse gas capture applications [11,12]. APTMS, a bifunctional silane, forms stable Si–O–Si bonds with hydroxylated surfaces, enabling uniform modification of inorganic matrices [13]. Its small molecular size facilitates penetration into fine pores. PEI, a polymer rich in primary, secondary, and tertiary amines, offers high adsorption capacity and performs well under humid conditions, where water promotes bicarbonate formation and prevents amine degradation [14–16].

The effectiveness of these agents varies with substrate type. APTMS is particularly suited to inorganic matrices, where it forms covalent bonds that resist leaching during adsorption–desorption cycles [8,13]. PEI, on the other hand, interacts with organic substrates via hydrogen bonding and physical adsorption, providing extensive surface coverage, albeit with less structural anchoring [14]. Thus, the choice of functionalizing agent must consider substrate compatibility, operational conditions, and regeneration requirements. Recent studies have demonstrated the efficacy of amine-functionalized waste materials. Zakria et al. [15] reported enhanced adsorption using various amines on coconut shell biochar, with triethylenetetramine (TETA) showing superior performance. Gholidoust et al. [16] achieved a 75% improvement in CO_2 capture by impregnating PEI onto mesoporous carbon derived from oil sands coke.

Another important factor to consider for these agro-industrial wastes to become industrially significant is their perishable nature or susceptibility to degradation during aggressive functionalization treatments. In the literature [17,18], aggressive pretreatments are commonly used to provide certain functional groups at the surface of some supports:

macerations, acid or basic hydrolysis, or heat-assisted extractions. Nevertheless, such methods tend to fragment the original structure of the material, dissolving functional compounds or generating degradation products. For example, organic acid pretreatments solubilize hemicellulose and part of lignin and generate low-molecular-weight products (e.g., monomeric sugars, furfurals, and phenolic fragments), which can compromise the integrity of the original solid and complicate downstream steps [17], while alkaline pretreatments saponify ester linkages and remove lignin, promoting structural fragmentation and mass loss of the solid phase [18].

Therefore, a more selective alternative can be established: direct functionalization with aminosilanes, APTMS and PEI over minimal processed wastes without high temperatures, which can be considered as a green alternative thanks to the elimination of aggressive reagents and solvents, such as concentrated alkaline solutions (NaOH or KOH), elimination of undesirable degradation products, and minimal energetic consumption. Therefore, this green alternative means that APTMS and PEI can be anchored through covalent bonds or by electrostatic forces, providing amine groups on the surface with the necessity to deconstruct the matrix [17].

Finally, beyond chemical reactivity, the success of an adsorbent in industrial applications is strongly conditioned by its behavior in packed beds. Properties such as bulk density, Carr Index, and Hausner Ratio determine powder flowability, packing homogeneity, and the likelihood of channeling or pressure drops. Thus, any evaluation of waste-derived adsorbents must integrate both their surface chemistry and their particulate flow properties to ensure practical applicability. For example, Rezaei [18] compared structured adsorbents with conventional particle beds and discussed how structured adsorbents can improve mass transfer and reduce pressure drop thanks to flow properties. Shah et al. [2] proposed accepted scales for Hausner's and Carr's indices and discussed how these metrics correlate with packed-bed density, ease of packing, and resistance to gas or liquid flow through the material during adsorption processes.

Therefore, the aim of this study is to evaluate the suitability of waste as functionalizable matrices and to compare the efficiency and compatibility of organic waste (corn cob, orange peel) with inorganic waste (eggshell and silica gel), considering that their physical and chemical properties can condition the success of amination with two different agents, APTMS and PEI, and their impact in flowability parameters that can impact directly on the adsorption process.

2. Materials and Methods

2.1. Reagents and Materials

3-Aminopropyltrimethoxysilane (APTMS, 97%, CAS 13822-56-5, Sigma-Aldrich, St. Louis, MO, USA) and branched polyethylenimine (PEI, average Mw ~25,000 by LS; average Mn ~10,000 by GPC; CAS 9002-98-6) were procured from Sigma-Aldrich (USA). Ethanol (absolute, analytical grade, A.C.S., MEYER 0390) served as the solvent for surface functionalization. Citric acid (anhydrous, 99.5–100.5%, JT Baker, CAS 77-92-9) was employed for surface activation of inorganic substrates. Hydrochloric acid (HCl, 37%, CAS 7647-01-0, Sigma-Aldrich) and sodium hydroxide (NaOH, pellets, CAS 1310-73-2, Sigma-Aldrich) were used for pH adjustment and Boehm titration analyses. All reagents were used as received, without further purification. Distilled water was utilized throughout all experimental procedures.

2.2. Preparation of Waste Substratres

2.2.1. Organic Waste

Orange peels and corn cobs were sourced from a local market in Orizaba, Mexico. The materials were thoroughly washed with distilled water to eliminate dirt and soluble residues. Following drying in a convection oven, the samples were milled to obtain fine particles: approximately 250 μm for orange peel (mesh #60) and 425 μm for corn cob (mesh #40).

2.2.2. Inorganic Waste

Eggshells (ESs), collected from domestic food waste, were washed, dried, and ground prior to use. Spent silica (WS), recovered from laboratory chromatography columns, was similarly processed. Both materials were washed with distilled water, dried at 60 °C for six hours until a constant mass was achieved, and subsequently milled to a particle size of approximately 150 μm (mesh #100). To enhance surface reactivity, inorganic matrices were subjected to acid activation using citric acid, a sustainable alternative aligned with the environmental objectives of this study. A 5% w/v citric acid solution was prepared by dissolving 5 g of citric acid in 100 mL of distilled water. Ten grams of either spent silica or ground eggshells was added to the solution and stirred continuously at 50 °C for one hour. The activated solids were then recovered, rinsed thoroughly with distilled water to remove residual acid, and dried at 60 °C until a constant weight was obtained.

2.3. Surface Functionalization

2.3.1. Functionalization with APTMS

Silanization using APTMS was performed in a glass vessel containing 20 g of each pulverized substrate and 120 mL of ethanol. The suspension was stirred at 400 rpm for 30 min to facilitate hydrolysis and improve reagent interaction. Subsequently, 2 mL of APTMS was added, and stirring continued for an additional three hours. Upon completion, the modified material was recovered, rinsed twice with distilled water to remove excess reagent, filtered, and dried at 60 °C until a constant mass was achieved.

2.3.2. Functionalization with PEI

PEI functionalization was conducted in a similar manner. Twenty grams of each pulverized substrate was suspended in 120 mL of distilled water and stirred at 400 rpm for 30 min. The pH of the suspension was adjusted to 8.5 using a 0.1 N NaOH solution to deprotonate the PEI and enhance its interaction with the substrate. A total of 250 μg of PEI was then added, and the mixture was stirred for three hours. The functionalized material was subsequently recovered, rinsed twice with distilled water, filtered, and dried at 60 °C until a constant weight was attained.

2.4. Characterization

2.4.1. Drying Kinetics Method

Drying kinetics were evaluated gravimetrically. Fresh samples of orange peel, corn cob, spent silica, and eggshell were dried under controlled conditions in a laboratory oven, with mass recorded at regular intervals until a constant weight was achieved. Moisture content (X_t) on dry basis for each time was calculated on a dry basis using Equation (1):

$$X_t = \frac{w - d}{d} \quad (1)$$

where w is wet weight of the sample for each determined time, while d is final dry weight of each sample. This equation measures how much water remains in the sample in relation to its dry mass.

Moisture ratio (MR) was determined using the final constant mass as the equilibrium moisture content. Drying behavior was modelled using the Page Equation (2):

$$MR = e^{-kt^n} \quad (2)$$

where k and n are empirical constants estimated via nonlinear least-squares regression.

2.4.2. Fourier-Transform Infrared (FTIR) Spectroscopy Method

Pristine, APTMS-functionalized, and PEI-functionalized samples of each matrix (orange peel, corn cob, spent silica, and eggshell) were analyzed using Fourier-Transform Infrared Spectroscopy (FTIR) on an Agilent Cary 630 spectrometer equipped with an attenuated total reflectance (ATR) accessory. A small quantity of each powder was placed directly on the ATR crystal, and spectra were recorded over the 600–5000 cm^{-1} range. This analysis enabled identification of characteristic functional groups associated with surface modification by APTMS and PEI.

2.4.3. ζ-Potential

Surface charge measurements were conducted using a Malvern Zetasizer Nano Series ZS90 particle analyzer. The ζ-potential, defined as the electrostatic potential between the particle surface and the surrounding ionic layer in aqueous suspension, was measured for both pristine and functionalized samples. This parameter provides insight into colloidal stability and confirms the incorporation of amine groups on the modified surfaces.

2.4.4. pH and Conductivity

To assess the interaction of the materials with aqueous media and infer surface modifications, pH and conductivity measurements were performed. For each sample, 10 mg of powder was dispersed in 10 mL of deionized water and stirred for 10 min. Measurements were taken at ambient temperature using a METTLER-TOLEDO 51302911m equipped with an LE438 probe. Variations in pH and conductivity before and after functionalization were used to infer the generation of new surface charges.

2.4.5. Boehm Titration: Quantification of Surface Acidic and Basic Groups

Boehm titration was employed to quantify acidic and basic functional groups on the surface of both pristine and modified matrices. This method enables evaluation of changes in surface acid–base character resulting from amine incorporation. For each test, 5 mg of dried sample was added to 10 mL of standardized acid (0.1 N HCl) or base (0.1 N NaOH) solution. After equilibration, the solutions were titrated with 0.1 N NaOH or 0.1 N HCl, respectively, using phenolphthalein as an indicator. Blank titrations were performed under identical conditions without solid material. The concentration of surface functional groups was calculated using the Equation (3):

$$meq/g = \frac{V\ blank - V\ sample}{m} \quad (3)$$

where V is the volume in mL, N is the normality in eq/L, and m is the sample mass in grams.

Two sets of titrations were conducted:

(a) In the first, excess HCl was used to quantify basic surface groups (e.g., amines, basic –OH sites, residual carbonates). The unreacted HCl was titrated with NaOH.

(b) Positive meq/g values indicate consumption of HCl by basic groups, while values near zero or negative suggest an absence of basic sites or experimental inconsistencies.

2.5. Applicability Assessment

To evaluate the flowability and compressibility of the particulate materials, the Carr Index (CI) and Hausner Ratio (HR) were determined. These parameters are critical for assessing the suitability of both pristine and functionalized matrices for use in packed-bed configurations, which are commonly employed in CO_2 capture systems.

Bulk density (ρ_a) was measured by gently pouring 4 mL (v_a) of powder into a pre-tared graduated glass cylinder and recording the mass (m) of the sample. Bulk density was calculated using Equation (4):

$$\rho_a = \frac{m}{v_a} \quad (4)$$

Bulk density (ρ_c) was subsequently determined by subjecting the cylinder containing the powder to 100 gentle drops from a height of 15 cm. The final volume (v_c) was recorded, and bulk density was calculated using Equation (5):

$$\rho_c = \frac{m}{v_c} \quad (5)$$

From these values, the Carr Index and Hausner Ratio were calculated to assess powder flowability and packing behaviour, using Equations (6) and (7):

$$IC = \frac{(\rho_c - \rho_a)}{\rho_c} \quad (6)$$

$$RH = \frac{\rho_c}{\rho_a} \quad (7)$$

These metrics provide insight into the handling characteristics of the materials and their potential performance in fixed-bed adsorption systems. According to Lebrun et al. [19], it is possible to classify flowability according to the Carr Index and Hausner Ratio, as presented in Table 1:

Table 1. Flowability classification [20] according to the Carr Index and Hausner Ratio.

Flowability	Carr Index (%)	Hausner Ratio
Excellent	0–10	1.00–1.11
Good	11–15	1.12–1.18
Fair	16–20	1.19–1.25
Passable	21–25	1.26–1.34
Poor	26–31	1.35–1.45
Very poor	32–37	1.46–1.59
Extremely poor	>38	>1.60

Lower CI and HR values are indicative of better flow properties, which are essential for efficient packing and adsorption applications.

3. Results and Discussion

3.1. Drying Kinetics

The drying behaviour of the evaluated residues revealed distinct patterns based on their organic or inorganic nature, as illustrated in Figure 1. In terms of moisture content (X_t), corn cob exhibited the highest initial water retention (~6 g/g) and the slowest drying rate, requiring over 300 min to reach equilibrium moisture. Orange peel, with a

lower initial moisture content (~3 g/g), displayed a moderately gradual drying curve, stabilizing after approximately 150 min. In contrast, the inorganic substrates, spent silica and eggshell, demonstrated minimal initial moisture (<1 g/g) and achieved equilibrium within 20 min, which can be attributed to their lower porosity and reduced content of hydrophilic functional groups, resulting in limited water retention capacity [21].

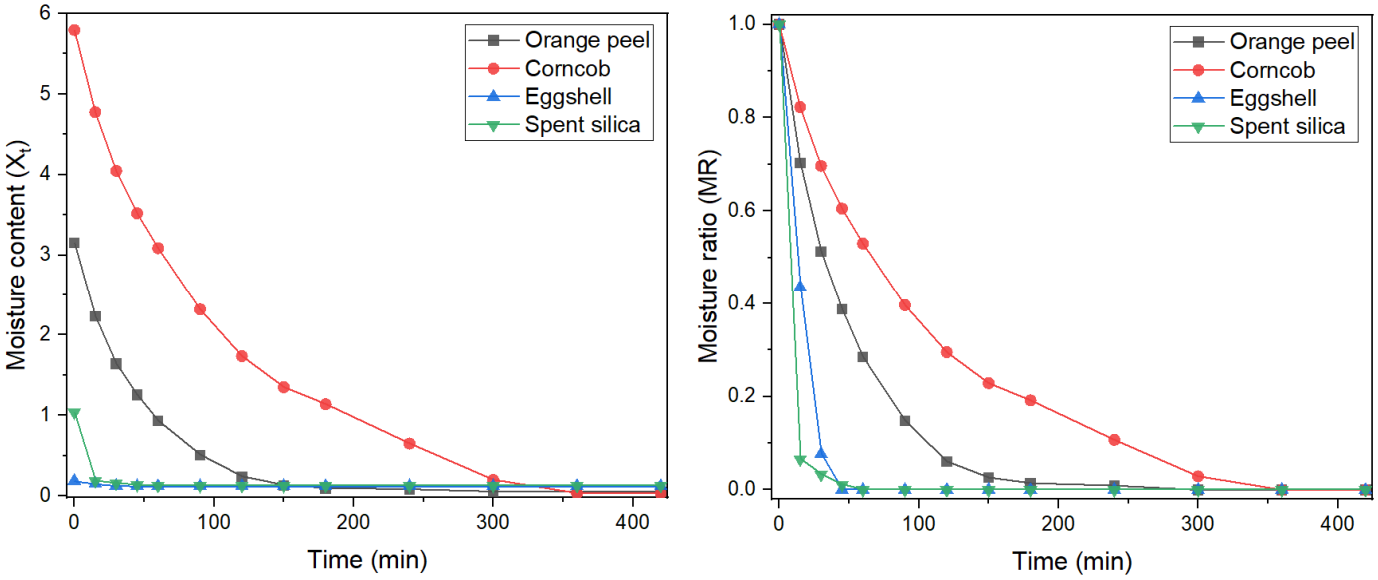


Figure 1. Drying kinetics for organic and inorganic waste.

Moisture ratio (MR) curves corroborated these observations: eggshell and spent silica showed a rapid decline in MR during the initial drying phase, whereas orange peel and corn cob underwent extended falling-rate periods. These results suggest that organic residues, owing to their porous architecture and abundance of hydrophilic functional groups (e.g., cellulose, hemicellulose, pectin), retain moisture more effectively. This property directly influences the energy requirements for pretreatment and conditioning prior to functionalization [21,22].

From a process engineering standpoint, residues with rapid drying kinetics, such as eggshell and silica, offer advantages in terms of energy efficiency and scalability, as they necessitate minimal drying time before chemical modification or integration into adsorption columns [9]. Conversely, materials with slower drying profiles, such as corn cob and orange peel, may require enhanced drying protocols, including increased airflow, mild thermal treatment, or pre-conditioning to facilitate moisture removal. In summary, drying kinetics not only reflect the intrinsic physical characteristics of the waste matrices but also bear practical implications for material preparation, operational costs, and adsorption efficiency [22].

These results are similar to those reported in the literature. Razola-Díaz et al. [23] found that orange peel has a moderately slow drying time and requires considerable time at low temperature. On the other hand, Pankaj et al. [24] worked with maize corn and found high initial humidity and a slow drying with a long falling-rate period with similar time to reach. Regarding inorganic waste, Souza et al. [25] analyzed the thin-film drying kinetics of silica gel at different temperatures (40–80 °C) and air velocities and observed that the moisture loss curves show a rapid initial phase followed by a more pronounced drop, with much shorter drying times than lignocellulosic materials. In terms of temperature and air velocities, we observed that the moisture loss curves show a rapid initial phase followed by a more pronounced drop, with much shorter drying times than lignocellulosic materials under favorable conditions.

3.2. Fourier-Transform Infrared (FTIR) Spectroscopy

The FTIR spectra of pristine orange peel (OP), APTMS-functionalized orange peel (OP–APTMS), and PEI-modified orange peel (OP–PEI) are presented in Figure 2. The spectrum of the unmodified OP displayed characteristic bands associated with lignocellulosic biomass: a broad O–H stretching vibration near 3400 cm^{-1}, aliphatic C–H stretching between 2920 and 2850 cm^{-1}, a carbonyl band around 1730 cm^{-1} (attributed to C=O stretching in hemicellulose and pectin esters), and intense C–O and C–O–C stretching vibrations in the 1240–1030 cm^{-1} region, indicative of polysaccharide structures [26].

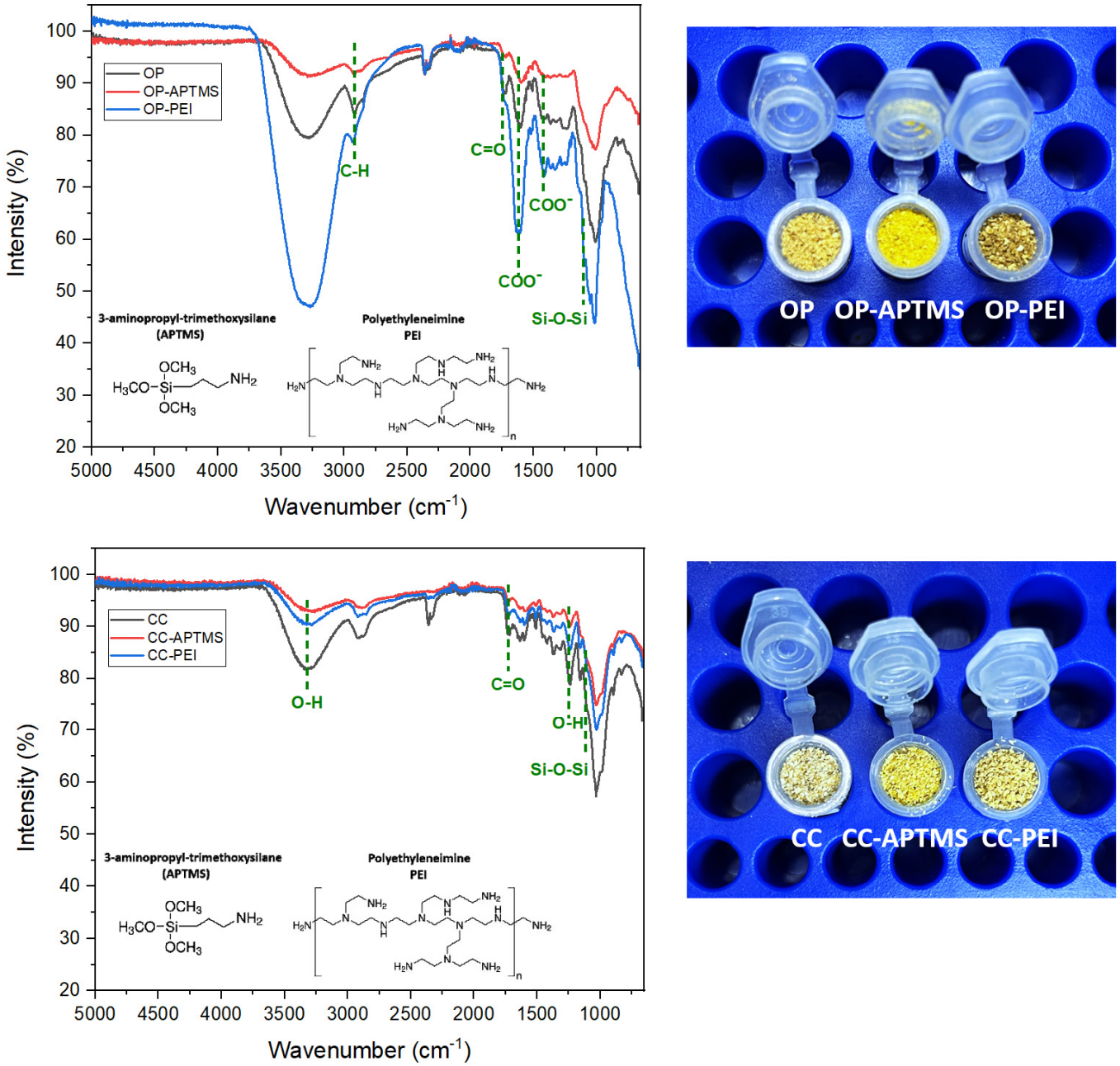


Figure 2. FTIR spectra for organic waste: orange peel (**up**) and corn cob (**down**).

Following APTMS functionalization for OP-APTMS, the spectrum revealed new features in the 3300–3400 cm^{-1} range, corresponding to N–H stretching vibrations, along with a slight increase in intensity at ~2930 cm^{-1}, associated with C–H stretching from propyl groups. Additionally, the region near 1100–1000 cm^{-1} showed enhanced absorption, consis-

tent with the formation of Si–O–Si and Si–O–C linkages [27]. These spectral modifications confirm the successful grafting of aminopropylsilane moieties onto the biomass surface.

In the case of OP–PEI, the broadening and increased intensity of the 3300–3400 cm^{-1} band reflects the superposition of O–H and abundant N–H stretching modes from the polymer. New bands appearing in the 1650–1560 cm^{-1} region are attributed to N–H bending and C–N stretching vibrations, further supporting the presence of PEI. The enhancement of aliphatic C–H stretching bands (2920–2850 cm^{-1}) also corroborates the deposition of PEI chains onto the substrate [28].

Collectively, these spectral changes provide clear evidence of the successful introduction of amino functionalities onto the surface of orange peel particles, consistent with the expected chemical modification pathways for both APTMS and PEI treatments.

The FTIR spectra of pristine corn cob (CC), APTMS-functionalized corn cob (CC–APTMS), and PEI-modified corn cob (CC–PEI) are presented in Figure 2. The spectrum of the unmodified CC exhibited characteristic absorptions typical of lignocellulosic biomass: a broad O–H stretching band near 3400 cm^{-1}, aliphatic C–H stretching between 2920 and 2850 cm^{-1}, and a carbonyl vibration around 1730 cm^{-1}, attributed to acetyl groups and ester linkages in hemicellulose. Additionally, aromatic skeletal vibrations of lignin were observed in the 1600–1510 cm^{-1} region, along with intense C–O and C–O–C stretching bands between 1240 and 1030 cm^{-1}, indicative of cellulose and hemicellulose structures [29].

Following APTMS functionalization, new spectral features emerged near 1100–1000 cm^{-1}, corresponding to Si–O–Si and Si–O–C vibrations, confirming the formation of siloxane linkages. An increase in intensity around 2930 cm^{-1} was observed, associated with the propyl chains of the silane, along with subtle contributions near 3300 cm^{-1} due to N–H stretching [27]. These modifications confirm the successful grafting of aminopropylsilane onto the biomass surface. In the case of CC–PEI, broadening and increased intensity in the 3300–3400 cm^{-1} region reflects the overlap of O–H and abundant N–H stretching vibrations from the polymer. Additional bands in the 1650–1560 cm^{-1} region were attributed to N–H bending and C–N stretching modes, while enhanced C–H stretching in the 2920–2850 cm^{-1} range further corroborates the deposition of PEI chains [28]. Overall, these spectral changes demonstrate the effective incorporation of amino functionalities onto corn cob particles, supporting their potential as chemically modified adsorbents with better selectivity.

The FTIR spectra of pristine eggshell (ES), APTMS-functionalized eggshell (ES–APTMS), and PEI-modified eggshell (ES–PEI) are presented in Figure 3. The spectrum of the unmodified ES displayed characteristic vibrational modes of calcium carbonate ($CaCO_3$), including strong absorptions in the 1415–870 cm^{-1} range, corresponding to asymmetric and out-of-plane bending of the carbonate ion (CO_3^{2-}), and a sharp band near 713 cm^{-1} attributed to in-plane bending. A broad band centred around 3430 cm^{-1} was assigned to O–H stretching from surface-adsorbed water, while a weaker signal near 2515 cm^{-1} is also typical of $CaCO_3$ [30].

Upon functionalization with APTMS, new spectral contributions emerged in the 1100–1000 cm^{-1} region, attributed to Si–O–Si and Si–O–C stretching vibrations, along with slight enhancements near 2930 cm^{-1} associated with the propyl groups of the silane [27]. In the case of ES–PEI, broadening and increased intensity in the 3400–3300 cm^{-1} region were observed, reflecting overlapping O–H and N–H stretching vibrations from the polymer. Additional bands in the 1650–1560 cm^{-1} region were assigned to N–H bending and C–N stretching, confirming the successful incorporation of polyethylenimine chains [28]. These spectral modifications indicate that both silane coupling and polymer functionalization were effective in generating amino-rich surfaces on eggshell particles, enhancing their suitability for adsorption applications.

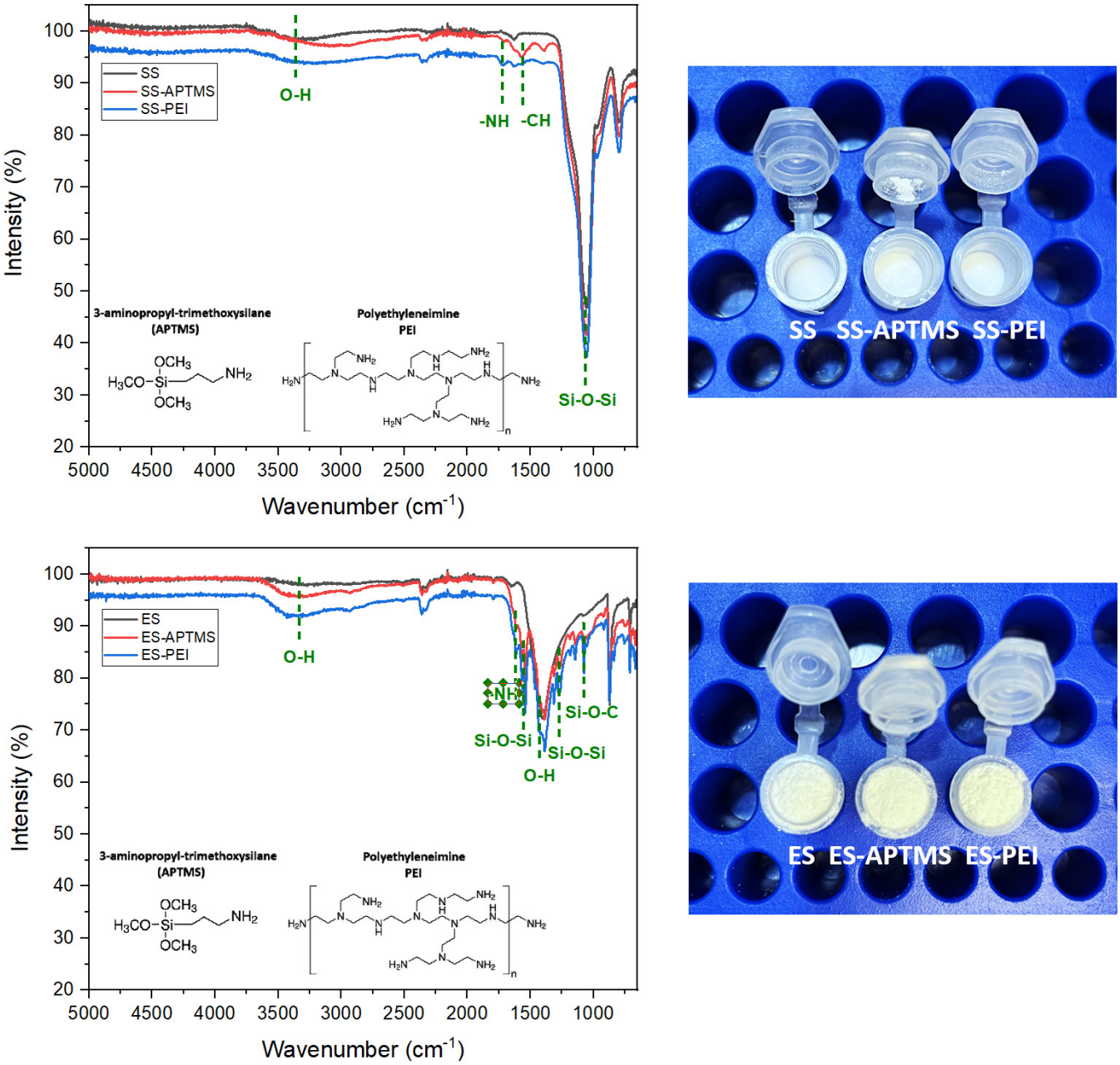


Figure 3. FTIR spectra for inorganic waste: eggshell (**up**) and spent silica (**down**).

The FTIR spectrum of pristine spent silica (SS) exhibited the characteristic bands of amorphous SiO_2: a strong asymmetric Si–O–Si stretching vibration near 1100 cm^{-1}, symmetric stretching around 800 cm^{-1}, and a bending vibration at approximately 460 cm^{-1}. A broad band centred at ~3430 cm^{-1} was attributed to O–H stretching of surface silanols and adsorbed water, with a corresponding H–O–H bending vibration near 1630 cm^{-1} [31].

Following APTMS functionalization (SS–APTMS), the spectrum showed increased intensity in the 1100–1000 cm^{-1} region, consistent with Si–O–Si and Si–O–C stretching from silane grafting. Weak C–H stretching bands near 2930 cm^{-1} confirmed the presence of propyl chains [27]. For the PEI-modified sample (SS–PEI), broad absorptions in the 3400–3300 cm^{-1} region were indicative of N–H stretching from primary and secondary amines. Additional signals in the 1650–1560 cm^{-1} region corresponded to N–H bending and C–N stretching vibrations, confirming the successful incorporation of polyamine groups onto the silica surface [28].

Taken together, the observed spectral changes across all matrices, organic (orange peel, corn cob) and inorganic (eggshell, spent silica), provide compelling evidence of successful chemical functionalization via amination. The presence of new functional groups, including Si–O–Si linkages from APTMS and amine-rich moieties from PEI, confirms the introduction of surface-active sites. These modifications are expected to enhance the affinity of the materials toward adsorption, fore example, for CO_2 capture through acid–base interactions and chemisorption mechanisms, thereby improving their performance in gas capture applications.

3.3. ζ-Potential

The ζ-potential measurements presented in Table 2 provide insight into the surface charge characteristics of both organic (orange peel and corn cob) and inorganic (eggshell and spent silica) matrices before and after functionalization with APTMS and PEI.

Table 2. Results of potential for organic and inorganic waste.

Sample	ζ Potential (mV)
Orange peel	−22.6
Orange peel-APTMS	−25.2
Orange peel-PEI	−29.1
Corn cob	−24.2
Corn cob-APTMS	−13.3
Corn cob-PEI	−19.0
Spent silica	−16.6
Spent silica-APTMS	−2.8
Spent silica-PEI	−19.4
Eggshell	−17.6
Eggshell-APTMS	−14.6
Eggshell-PEI	−9.8

3.3.1. Organic Substrates ζ-Potential

Pristine orange peel and corn cob exhibited moderately negative ζ-potential values (−22.6 mV and −24.2 mV, respectively), indicative of deprotonated hydroxyl and carboxyl groups inherent to lignocellulosic biomass. Upon functionalization with APTMS, the ζ-potential of orange peel shifted slightly to −25.2 mV, while corn cob showed a less negative value of −13.3 mV. These changes suggest that the difference is due to the intrinsic chemistry of each biomass. In contrast, PEI affected the ζ-potential in a matrix-dependent manner. In orange peel, the value was more negative (−29.1 mV), while in corn cob, it was less negative (−19.0 mV). The change in values was expected due to the presence of protonated amine groups (–NH_2/–NH) introduced by the polymer, which partially neutralize the native negative charge [32]. But the contrasting behavior in ζ-potential shifts after APTMS functionalization can be explained by differences in the surface chemistry and accessibility of functional groups in each biomass, as identified in the FTIR spectra in Section 3.2. Orange peel is rich in pectin and soluble phenolic compounds that contain carboxylic groups (1730–1700, 1610–1550, and 1410–1380 cm^{-1}), which tend to remain exposed even after silanization. As a result, the grafting of APTMS on orange peel surfaces may leave a fraction of negatively charged carboxylates unneutralized, leading to a slight increase in negative ζ-potential. In contrast, corn cob contains a higher proportion of cellulose and lignin, where hydroxyl groups (3600–3000 and 1330–1260 cm^{-1}) are the dominant reactive sites [26–28]. For this material, the introduction of silane groups from APTMS partially masks or substitutes surface hydroxyls, reducing the density of exposed

deprotonated oxygen species. Consequently, the overall surface charge becomes less negative. This highlights that the net ζ-potential shift depends not only on the chemistry of the modifying agent but also on the relative abundance and accessibility of native surface functionalities in each substrate. PEI generally tends to neutralize negative surface charges through protonated amines; however, in OP, the high density of carboxylates leads to stronger ionic interactions, shifting the ζ-potential to more negative values.

3.3.2. Inorganic Substrates ζ-Potential

Spent silica initially displayed a ζ-potential of −16.6 mV, consistent with the presence of surface silanol groups. APTMS functionalization significantly reduced the magnitude to −2.8 mV, reflecting silane condensation and partial neutralization of surface hydroxyls. PEI-modified silica showed a ζ-potential of −19.4 mV, suggesting a balance between residual silanols and protonated amines [33]. Eggshell, composed primarily of calcium carbonate, exhibited an initial ζ-potential of −17.6 mV. Functionalization with APTMS resulted in a modest shift to −14.6 mV, while PEI treatment further reduced the magnitude to −9.8 mV. These trends indicate progressive surface coverage by organosilane and polyamine layers, diminishing the availability of negatively charged carbonate and hydroxyl groups [34,35].

3.4. Acid–Base Properties

The acid–base characteristics of the pristine and functionalized matrices were evaluated via Boehm titration, with results summarized in Table 3. Meq/g values were calculated using Equation (3), where positive values indicate HCl consumption due to the presence of basic surface groups, and negative values suggest the absence of such groups or experimental limitations [36].

Table 3. Results of acid–base properties.

Sample	Titration		pH	Electric Potential (mV)	Conductivity (mS/cm)
	Acid Type (Meq/g)	Basic Type (Meq/g)			
Orange peel	-1.92×10^{-5}	3.50×10^{-5}	5.35	130	0.008
Orange peel-APTMS	2.87×10^{-6}	2.50×10^{-5}	5.34	117	0.009
Orange peel-PEI	4.76×10^{-6}	2.00×10^{-5}	5.40	114	0.012
Corn cob	1.10×10^{-5}	3.50×10^{-5}	6.10	7.3	0.018
Corn cob-APTMS	-1.01×10^{-5}	-3.50×10^{-6}	7.77	−16	0.015
Corn cob-PEI	-3.64×10^{-6}	-3.00×10^{-6}	5.85	30	0.014
Spent silica	-1.00×10^{-5}	6.00×10^{-5}	7.24	7	0.020
Spent silica-APTMS	-7.00×10^{-6}	2.00×10^{-5}	4.87	144	0.013
Spent silica-PEI	-2.01×10^{-6}	3.00×10^{-5}	4.40	171	0.016
Eggshell	4.04×10^{-6}	4.00×10^{-5}	10.09	−156	0.024
Eggshell-APTMS	1.55×10^{-5}	4.00×10^{-5}	9.80	−140	0.023
Eggshell-PEI	1.27×10^{-5}	1.67×10^{-5}	9.52	−124	0.022

According to Table 3, different behavior was found for the four matrices, when each was functionalized with a different amine agent and depending on the titration type.

3.4.1. Organic Substrates Titration Value

Pristine orange peel exhibited a slightly negative acid-type titration value (-1.92×10^{-5} meq/g), indicating a predominance of acidic functional groups such as carboxyls and phenols. Functionalization with APTMS resulted in a modest increase (2.87×10^{-6} meq/g), suggesting limited incorporation of amino groups. PEI treatment further increased the value to 4.76×10^{-6} meq/g, reflecting a higher density of accessible

amines. In basic-type titration, all orange peel samples showed negligible values, consistent with the dominance of acidic groups and limited basic site availability. Corn cob samples, both pristine and functionalized, yielded negative values in acid-type titration (up to -3.64×10^{-6} meq/g), indicating an absence of measurable basic groups. This may be attributed to low coupling efficiency, site blockage by residual lignin, or high experimental variability due to poor solubility [37,38].

3.4.2. Inorganic Substrates Titration Value

Pristine spent silica showed values near zero, as expected for a material dominated by acidic silanol groups [35]. APTMS-functionalized silica exhibited a slightly negative value (-7.00×10^{-6} meq/g), likely due to insufficient amine incorporation. PEI-modified silica also showed a negative value (-2.01×10^{-6} meq/g), suggesting poor polymer retention or quantification challenges. Eggshell, composed primarily of calcium carbonate, demonstrated a relatively high basicity (4.04×10^{-6} meq/g), consistent with its alkaline nature. APTMS treatment reduced this value to 1.55×10^{-6} meq/g, likely due to surface coverage by silane groups. PEI functionalization restored and enhanced the basicity (1.27×10^{-5} meq/g), confirming the effective introduction of accessible amines [39,40]. According to the results, it is possible to recognize the limitations of the method (solubility, low density of accessible groups, quantification errors); nevertheless, some trends were observed in the introduction of basic groups with PEI and partial incorporation with APTMS, consistent with the expected surface chemistry

3.4.3. pH, Electric Potential, and Conductivity

Table 3 also presents pH, electric potential, and conductivity data, which reflect changes in acid–base behaviour, charge distribution, and ionic exchange properties following functionalization. For organic residues, pH values ranged from slightly acidic to near neutral. Orange peel maintained an acidic profile (pH 5.34–5.40) even after modification, consistent with the persistence of organic acids. Corn cob exhibited higher pH values (6.10–7.77), particularly after APTMS treatment, suggesting partial neutralization of acidic groups. Inorganic residues displayed distinct trends. Pristine spent silica had a neutral pH (7.24), which decreased to acidic levels after functionalization (pH 4.87 with APTMS, 4.40 with PEI), reflecting the influence of introduced silanol and amine groups. Eggshell, dominated by $CaCO_3$, exhibited alkaline pH values (9.52–10.09), which were only slightly reduced after modification, indicating the buffering capacity of the carbonate system.

According to the above, the acidic nature of both functionalizations influenced the observed pH values across the evaluated matrices. Inorganic substrates such as spent silica and eggshell were first subjected to citric acid activation, which introduced surface –OH and –COOH groups while also leaving adsorbed acidic residues that lowered the suspension pH after functionalization. This effect was particularly evident in silica, which shifted from neutral (pH 7.24) to acidic values (pH 4.87 with APTMS and 4.40 with PEI). In contrast, eggshell maintained alkaline pH values (9.52–10.09) due to the buffering capacity of $CaCO_3$, though a slight decrease was observed after modification, consistent with the partial coverage of carbonate sites. For organic residues, the persistence of intrinsic carboxylic acids in orange peel explained its consistently acidic profile (~5.3–5.4), whereas corn cob showed an increase in pH after APTMS treatment (7.77), likely due to neutralization or masking of acidic groups by silane linkages [41].

Electric potential measurements revealed that orange peel maintained high positive values (~130 mV), which decreased slightly after functionalization but remained strongly positive, suggesting high proton mobility. Corn cob showed low or negative potentials (7.3 mV pristine, −16 mV with APTMS) but shifted to +30 mV after PEI treatment, indi-

cating an enhanced cationic character. Spent silica showed a similar trend, with pristine material near neutral (7 mV), increasing to +144 mV (APTMS) and +171 mV (PEI), confirming strong surface modification. Eggshell exhibited strongly negative potentials (−156 to −124 mV), consistent with carbonate surfaces, with slight reductions after functionalization. Conductivity measurements indicated that organic residues maintained low ionic conductivities (0.008–0.018 mS/cm), while inorganic residues exhibited higher values (0.013–0.024 mS/cm), reflecting greater ionic release. PEI functionalization consistently increased conductivity, attributable to protonated amines and enhanced ionic mobility.

These findings demonstrate that surface functionalization significantly alters the acid–base behaviour, charge distribution, and ionic exchange properties of both organic and inorganic matrices. Furthermore, the pH after functionalization depends on the substrate and pre-activation (e.g., citrate in inorganic materials can acidify), so there is no universal trend toward more alkaline values with APTMS.

3.5. Flow Properties

The flowability analysis revealed distinct differences between organic and inorganic residues, primarily influenced by their particle packing behaviour. Table 4 summarizes the results derived from Equations (4)–(7), and flowability classifications were assigned based on the criteria established by Lebrun et al. [19].

Table 4. Results of flow properties.

Sample	Carr Index (%)	Hausner Ratio	Flowability [21]
Orange peel	25	1.33	Passable
Orange peel-APTMS	20	1.25	Passable
Orange peel-PEI	10	1.11	Excellent
Corn cob	10	1.11	Excellent
Corn cob-APTMS	15	1.18	Good
Corn cob-PEI	10	1.11	Excellent
Spent silica	30	1.43	Poor
Spent silica-APTMS	20	1.25	Fair
Spent silica -PEI	23	1.29	Passable
Eggshell	13	1.14	Good
Eggshell-APTMS	25	1.33	Passable
Eggshell-PEI	23	1.29	Passable

3.5.1. Organic Substrates Carr Index

Corn cob exhibited the most favourable flow properties, with Carr Index (CI) values ranging from 10 to 15% and Hausner Ratios (HRs) close to 1.11, corresponding to “excellent” to “good” flowability. These results suggest that corn cob particles achieve homogeneous packing with minimal interparticle friction, promoting uniform gas distribution and reducing pressure drop in packed-bed adsorption systems. Orange peel demonstrated higher CI values (20–25%) and HR values up to 1.33, classified as “passable.” However, functionalization with PEI improved its flowability (CI = 10%, HR = 1.11), enhancing its suitability for stable operation in adsorption columns.

3.5.2. Inorganic Substrates Carr Index

Eggshell exhibited “good” flowability (CI = 11–15%), and the functionalization with APTMS and PEI even decreased the flowability to passable HR (1.33 and 1.29, respectively). This may result in increased channeling and non-uniform packing in reactors, potentially reducing adsorption efficiency. While spent silica powders displayed the poorest flow

characteristics (CI = 30%, HR = 1.43), classified as "poor", and although the functionalization improves flowability to "fair and passable, the overall flow properties remained inferior to those of the organic matrices [2,19]. These values indicate high cohesiveness and low packing uniformity, which could hinder reproducibility in adsorption experiments by increasing bed compaction and limiting effective gas–solid contact.

3.5.3. Process Implications

From an engineering perspective, materials with "excellent" to "good" flowability, such as corn cob and PEI-functionalized orange peel, are more suitable for packed-bed adsorption systems. Their favourable packing behaviour can ensure stable pressure profiles, uniform molecule diffusion, and optimal utilization of adsorption sites. In contrast, materials with poor flowability (e.g., eggshell and unmodified silica) may require additional pretreatment strategies, such as particle size optimization, granulation, or blending with flow-enhancing agents, to be viable in large-scale reactor applications. Overall, the results demonstrate that surface functionalization not only anchors the amine agents to improve selectivity and affinity for certain species but also improves particle flow behaviour, an essential consideration for scaling materials from batch testing to continuous packed-bed systems [2,19].

4. Conclusions

This study demonstrated the feasibility of functionalizing organic (orange peel, corn cob) and inorganic (spent silica, eggshell) waste matrices with 3-aminopropyltrimethoxysilane (APTMS) and polyethylenimine (PEI) for applications in CO_2 capture systems. Characterization via FTIR spectroscopy, ζ-potential analysis, and physicochemical assays confirmed the successful incorporation of amine functionalities across all substrates.

Organic matrices, particularly orange peel and corn cob, exhibited higher surface reactivity and underwent more pronounced chemical modification following functionalization, benefiting from their porous and hydrophilic lignocellulosic structures. However, these materials also displayed slower drying kinetics and variable flow properties, which may affect packing efficiency in reactor systems. In contrast, inorganic matrices such as spent silica and eggshell demonstrated faster drying rates and greater dimensional stability, facilitating processing and integration into adsorption systems. Notably, spent silica responded favourably to PEI functionalization despite its initially low surface charge, while eggshell, although limited by its inherent alkalinity, showed substantial modification potential.

Regarding the functionalizing agents, APTMS enabled covalent bonding with hydroxylated surfaces, forming stable silane layers, particularly effective in silica and eggshell matrices, though with moderate amine density. PEI can impart a higher concentration of active sites, as evidenced by ζ-potential and conductivity, but also tended to reduce powder flowability, potentially introducing diffusional limitations when used in excess.

Among the systems evaluated, orange peel–PEI and corn cob–APTMS emerged as the most promising organic matrices, while spent silica–PEI demonstrated better performance among inorganic supports. These findings underscore the importance of tailoring the choice of functionalizing agent and substrate to balance surface chemistry, processing feasibility, and reactor performance. Such optimization is essential for advancing the development of low-cost, sustainable sorbents within circular economy frameworks.

Future Work and Scalability Considerations

While the present study confirms the viability of amine-functionalized waste matrices, further research is needed to evaluate long-term stability, regeneration efficiency, and performance under dynamic flow conditions, especially in CO_2 capture. Scaling these materials

for industrial applications will require optimization of functionalization protocols to ensure reproducibility, cost-effectiveness, and minimal environmental impact. Additionally, integration into modular packed-bed systems and assessment under real flue gas compositions will be essential to validate their operational robustness and commercial potential.

Author Contributions: Conceptualization, A.M.B. and A.M.-S.; methodology, A.M.B., M.G.P.-J. and R.P.-G.; software, J.P.R.-J.; validation, J.P.R.-J. and A.A.-L.; formal analysis, M.G.P.-J.; investigation, A.M.B., M.G.P.-J. and J.P.R.-J.; data curation, M.G.P.-J.; writing—original draft, A.M.B. and M.G.P.-J.; writing—review and editing, A.M.B. and A.M.-S.; supervision, A.M.B., A.M.-S. and R.P.-G.; funding acquisition, R.P.-G. All authors have read and agreed to the published version of the manuscript.

Funding: This research received no external funding.

Data Availability Statement: The original contributions presented in this study are included in the article. Further inquiries can be directed to the corresponding authors.

Acknowledgments: This work was supported by the Secretaría de Ciencia, Humanidades, Tecnología e Innovación (SECIHTI) and the Tecnológico Nacional de México (TecNM). We gratefully acknowledge their financial contribution to this paper.

Conflicts of Interest: The authors declare no conflicts of interest.

References

1. Wang, Q.; Luo, J.; Zhong, Z.; Borgna, A. CO_2 capture by solid adsorbents and their applications: Current status and new trends. *Energy Environ. Sci.* **2011**, *4*, 42–55. [CrossRef]
2. Shah, D.S.; Moravkar, K.K.; Jha, D.K.; Lonkar, V.; Amin, P.D.; Chalikwar, S.S. A concise summary of powder processing methodologies for flow enhancement. *Heliyon* **2023**, *9*, e16498. [CrossRef] [PubMed]
3. Samanta, A.; Zhao, A.; Shimizu, G.K.H.; Sarkar, P.; Gupta, R. Post-combustion CO_2 capture using solid sorbents: A review. *Ind. Eng. Chem. Res.* **2012**, *51*, 1438–1463. [CrossRef]
4. Nugent, P.; Belmabkhout, Y.; Burd, S.D.; Cairns, A.J.; Luebke, R.; Forrest, K.; Pham, T.; Ma, S.; Space, B.; Wojtas, L.; et al. Porous materials with optimal adsorption thermodynamics and kinetics for CO_2 separation. *Nature* **2013**, *495*, 80–84. [CrossRef]
5. IPCC. *Climate Change 2021: The Physical Science Basis. Contribution of Working Group I to the Sixth Assessment Report of the Intergovernmental Panel on Climate Change*; Cambridge University Press: Cambridge, UK, 2021.
6. Pachauri, R.K.; Allen, M.R.; Barros, V.R.; Broome, J.; Cramer, W.; Christ, R.; Church, J.A.; Clarke, L.; Dahe, Q.; Dasgupta, P.; et al. *Climate Change 2014: Synthesis Report*; IPCC: Geneva, Switzerland, 2014.
7. de Quadros Melo, D.; de Oliveira Sousa Neto, V.; de Freitas Barros, F.C.; Raulino, G.S.C.; Vidal, C.B.; do Nascimento, R.F. Chemical modifications of lignocellulosic materials and their application for removal of cations and anions from aqueous solutions. *J. Appl. Polym. Sci.* **2016**, *133*, 1–22. [CrossRef]
8. Singh, D.; Kumar, R.; Kumar, A.; Rai, K.N. Synthesis and characterization of rice husk silica, silica-carbon composite and H_3PO_4 activated silica. *Ceramica* **2008**, *54*, 203–212. [CrossRef]
9. Wegman, R.F.; van Twisk, J. *Surface Preparation Techniques for Adhesive Bonding*, 2nd ed.; Elsevier Science: Amsterdam, The Netherlands, 2012; pp. 31–35, 48–49.
10. Bae, J.Y.; Jang, S.G.; Cho, J.; Kang, M. Amine-Functionalized Mesoporous Silica for Efficient CO_2 Capture: Stability, Performance, and Industrial Feasibility. *Int. J. Mol. Sci.* **2025**, *26*, 4313. [CrossRef]
11. Choi, S.; Drese, J.H.; Jones, C.W. Adsorbent materials for carbon dioxide capture from large anthropogenic point sources. *ChemSusChem Chem. Sustain. Energy Mater.* **2009**, *2*, 796–854. [CrossRef]
12. Didas, S.A.; Choi, S.; Chaikittisilp, W.; Jones, C.W. Amine–oxide hybrid materials for CO_2 capture from ambient air. *Acc. Chem. Res.* **2015**, *48*, 2680–2687. [CrossRef]
13. Tonle, I.K.; Diaco, T.; Ngameni, E.; Detellier, C. Nanohybrid kaolinite-based materials obtained from the interlayer grafting of 3-aminopropyltriethoxysilane and their potential use as electrochemical sensors. *Chem. Mater.* **2007**, *19*, 6629–6636. [CrossRef]
14. Gómez-Pozuelo, G.; Sanz-Pérez, E.S.; Arencibia, A.; Pizarro, P.; Sanz, R.; Serrano, D.P. CO_2 adsorption on amine-functionalized clays. *Microporous Mesoporous Mater.* **2019**, *282*, 38–47. [CrossRef]
15. Zakaria, D.S.; Rozi, S.K.M.; Halim, H.N.A.; Mohamad, S.; Zheng, G.K. New porous amine-functionalized biochar-based desiccated coconut waste as efficient CO_2 adsorbents. *Environ. Sci. Pollut. Res.* **2024**, *31*, 16309–16327. [CrossRef] [PubMed]

16. Gholidoust, A.; Atkinson, J.D.; Hashisho, Z. Enhancing CO_2 adsorption via amine-impregnated activated carbon from oil sands coke. *Energy Fuels* **2017**, *31*, 1756–1763. [CrossRef]
17. Oriez, V.; Peydecastaing, J.; Pontalier, P.Y. Lignocellulosic biomass fractionation by mineral acids and resulting extract purification processes: Conditions, yields, and purities. *Molecules* **2019**, *24*, 4273. [CrossRef]
18. Rezaei, F. Optimization of Structured Adsorbents for Gas Separation Processes. Ph.D. Thesis, Department of Chemical Engineering Monash University, Melbourne, Australia, 2011.
19. Lebrun, P.; Krier, F.; Mantanus, J.; Grohganz, H.; Yang, M.; Rozet, E. Design space approach in the optimization of the spray-drying process. *Eur. J. Pharm. Biopharm.* **2012**, *80*, 226–234. [CrossRef]
20. Maurya, D.P.; Singla, A.; Negi, S. An overview of key pretreatment processes for biological conversion of lignocellulosic biomass to bioethanol. *3 Biotech* **2015**, *5*, 597–609. [CrossRef]
21. Ioannidou, O.; Zabaniotou, A. Agricultural residues as precursors for activated carbon production—A review. *Renew. Sustain. Energy Rev.* **2007**, *11*, 1966–2005. [CrossRef]
22. Abolore, R.S.; Jaiswal, S.; Jaiswal, A.K. Green and sustainable pretreatment methods for cellulose extraction from lignocellulosic biomass and its applications: A review. *Carbohydr. Polym. Technol. Appl.* **2024**, *7*, 100396. [CrossRef]
23. Razola-Díaz, M.D.C.; Verardo, V.; Gómez-Caravaca, A.M.; García-Villanova, B.; Guerra-Hernández, E.J. Mathematical modelling of convective drying of orange by-product and its influence on phenolic compounds and ascorbic acid content, and its antioxidant activity. *Foods* **2023**, *12*, 500. [CrossRef]
24. Pankaj, K.; Dhritiman, S. Drying kinetics of maize cob using mathematical modelling. *J. Agric. Eng.* **2021**, *58*, 40–49. [CrossRef]
25. Souza, G.F.M.V.; Miranda, R.F.; Arruda, E.B.; Mendoza, O.S.; Barrozo, M.A. Drying kinetics of silica gel: Statistical discrimination using nonlinearity measures. *Chem. Eng. Technol.* **2012**, *35*, 797–802. [CrossRef]
26. Yaradoddi, J.S.; Banapurmath, N.R.; Ganachari, S.V.; Soudagar, M.E.M.; Sajjan, A.M.; Kamat, S.; Mujtaba, M.; Shettar, A.S.; Anqi, A.E.; Safaei, M.R.; et al. Bio-based material from fruit waste of orange peel for industrial applications. *J. Mater. Res. Technol.* **2022**, *17*, 3186–3197. [CrossRef]
27. Haniffa, M.A.C.M.; Ching, Y.C.; Chuah, C.H.; Ching, K.Y.; Liou, N.S. Synergistic effect of (3-Aminopropyl) Trimethoxysilane treated ZnO and corundum nanoparticles under UV-irradiation on UV-cutoff and IR-absorption spectra of acrylic polyurethane based nanocomposite coating. *Polym. Degrad. Stab.* **2019**, *159*, 205–216. [CrossRef]
28. Jiang, W.; Xing, Y.; Mo, L.; Liao, J.; Chen, W.; Wang, H.; Wang, T. Synthesis of polyethylenimine modified sugarcane bagasse cellulose and its competitive adsorption of Pb^{2+}, Cu^{2+} and Zn^{2+} from aqueous solutions. *Desalination Water Treat.* **2022**, *270*, 172–184. [CrossRef]
29. Xu, F.; Yu, J.; Tesso, T.; Dowell, F.; Wang, D. Qualitative and quantitative analysis of lignocellulosic biomass using infrared techniques: A mini-review. *Appl. Energy* **2013**, *104*, 801–809. [CrossRef]
30. Awogbemi, O.; Vandi, D.; Aigbodion, V. Pathways for sustainable utilization of waste chicken eggshell. *J. Renew. Mater.* **2022**, *10*, 2217. [CrossRef]
31. Vansant, E.F.; Van Der Voort, P.; Vrancken, K.C. Chapter 3 The surface chemistry of silica. *Stud. Surf. Sci. Catal.* **1995**, *93*, 59–77. [CrossRef]
32. Zwawi, M. A review on natural fiber bio-composites, surface modifications and applications. *Molecules* **2021**, *26*, 404. [CrossRef]
33. Zhuravlev, L.T. The surface chemistry of amorphous silica. Zhuravlev model. *Colloids Surf. A Physicochem. Eng. Asp.* **2000**, *173*, 1–38. [CrossRef]
34. Al Mahrouqi, D.; Vinogradov, J.; Jackson, M.D. Zeta potential of artificial and natural calcite in aqueous solution. *Adv. Colloid Interface Sci.* **2017**, *240*, 60–76. [CrossRef]
35. Perera, H.J.; Mortazavian, H.; Blum, F.D. Surface properties of silane-treated diatomaceous earth coatings: Effect of alkyl chain length. *Langmuir* **2017**, *33*, 2799–2809. [CrossRef]
36. Boehm, H.P. Surface oxides on carbon and their analysis: A critical assessment. *Carbon* **2002**, *40*, 145–149. [CrossRef]
37. Yan, J.; Oyedeji, O.; Leal, J.H.; Donohoe, B.S.; Semelsberger, T.A.; Li, C.; Hoover, A.N.; Webb, E.; Bose, E.A.; Zeng, Y.; et al. Characterizing variability in lignocellulosic biomass: A review. *ACS Sustain. Chem. Eng.* **2020**, *8*, 8059–8085. [CrossRef]
38. Wu, Y.; Cao, F.; Jiang, H.; Zhang, Y. Preparation and characterization of aminosilane-functionalized cellulose nanocrystal aerogel. *Mater. Res. Express* **2017**, *4*, 085303. [CrossRef]
39. Manzano, J.S.; Wang, H.; Kobayashi, T.; Naik, P.; Lai, K.C.; Evans, J.W.; Slowing, I.I. Kinetics of the functionalization of mesoporous silica nanoparticles: Implications on surface group distributions, adsorption and catalysis. *Microporous Mesoporous Mater.* **2020**, *305*, 110276. [CrossRef]

40. Beagan, A.; Alotaibi, K.; Almakhlafi, M.; Algarabli, W.; Alajmi, N.; Alanazi, M.; Alwaalah, H.; Alharbi, F.; Alshammari, R.; Alswieleh, A. Amine and sulfonic acid functionalized mesoporous silica as an effective adsorbent for removal of methylene blue from contaminated water. *J. King Saud Univ.-Sci.* **2022**, *34*, 101762. [CrossRef]
41. Rostami, M.; Mohseni, M.; Ranjbar, Z. Investigating the effect of pH on the surface chemistry of an amino silane treated nano silica. *Pigment Resin Technol.* **2011**, *40*, 363–373. [CrossRef]

Disclaimer/Publisher's Note: The statements, opinions and data contained in all publications are solely those of the individual author(s) and contributor(s) and not of MDPI and/or the editor(s). MDPI and/or the editor(s) disclaim responsibility for any injury to people or property resulting from any ideas, methods, instructions or products referred to in the content.